

P9.1 AIRBORNE DOPPLER RADAR OBSERVATIONS OF A SHALLOW COLD FRONT

Huaqing Cai* and Roger M. Wakimoto
Department of Atmospheric Sciences
UCLA
Los Angeles, CA 90095-1565

1. INTRODUCTION

A classical example of frontogenesis presented in textbooks is one that is produced by a deformation field (e.g., Holton 1992). Horizontal stretching deformation tends to advect the temperature field so that the isotherms become concentrated along the axis of dilation, provided that the temperature field has a gradient along the axis of contraction. This type of frontogenesis has resulted in a number of theoretical investigations (e.g., Davis and Müller 1988) but a surprising dearth of observational studies. The only detailed analysis known to the authors is by Ostdiek and Blumen (1995) using data collected during STORM-FEST. The primary data platforms used in their study were a dense surface mesonet and upper-air data from rawin-sondes and the NOAA demonstration profiler network.

On 26 January 1997, a front located within a horizontal deformation field was sampled by ELDORA (Electra Doppler Radar). High-resolution dual-Doppler winds and detailed thermodynamic fields were used to recreate the horizontal and vertical structure of the front.

2. SURFACE ANALYSIS

A surface analysis of sea-level pressure and potential temperature is shown in Fig. 1. The frontal position is supported by the gradient of the isentropes and streamlines shown in Figs. 1b and 2, respectively. It is analyzed as a cold front owing to its movement of 5.9 ms^{-1} from 305° . The Electra collected data near the col or saddle point defined by the two high and low pressure patterns shown in Figs. 1a and 2.

An objective analysis of the frontogenesis is plotted in Fig. 2 and reveals weak positive values in the area sampled by the aircraft. Much stronger values $\sim 30 \times 10^{-1} \text{ K}/100 \text{ km/h}$ are plotted to the south. A plot of frontogenesis at 1800 UTC (not shown) revealed that the front had undergone weak frontogenesis for the preceding 6 hours. A time series of the in situ winds at 600 m MSL in Fig. 3 reveals a sharp wind shift and significant cooling of $\sim 6 \text{ K}$ in virtual potential temperature (θ_v).

An enlargement of the θ_v field at low levels combined with dual-Doppler and in situ winds is presented

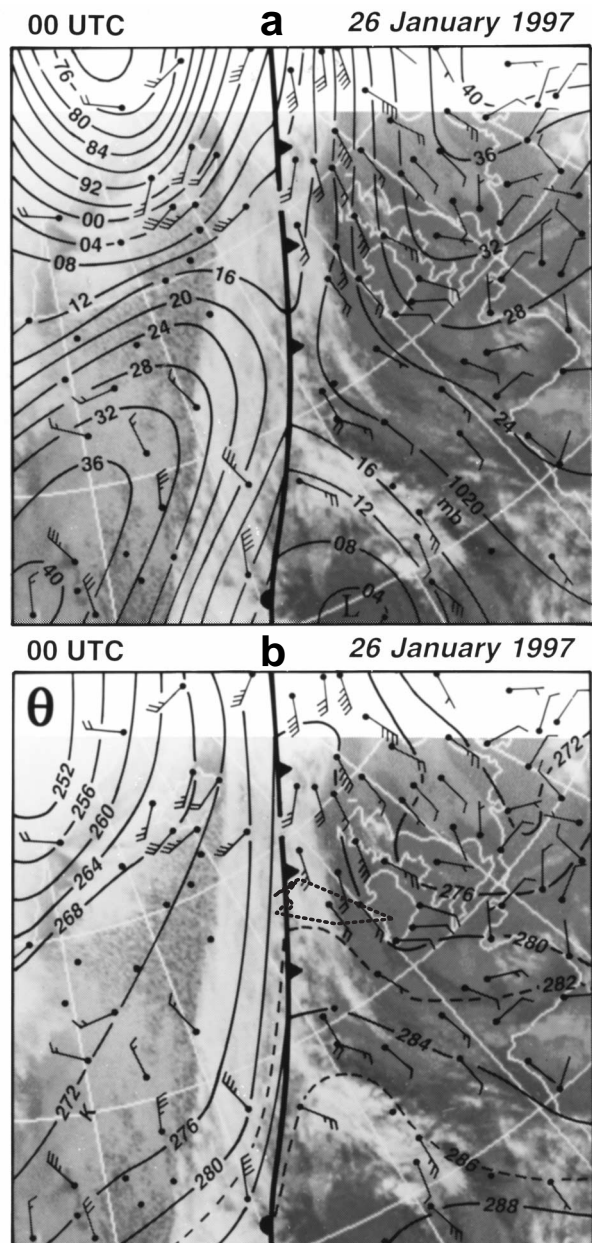


Fig. 1. a) Sea-level pressure analysis superimposed on an infrared satellite image at 00 UTC 26 January 1997. b) Isentropic analysis superimposed on the same image. The short-dashed line in b) represents the flight track of the Electra.

* Corresponding author address: Huaqing Cai, UCLA, Dept. of Atmospheric Sciences, Los Angeles, CA 90095-1565; e-mail: caihq@atmos.ucla.edu

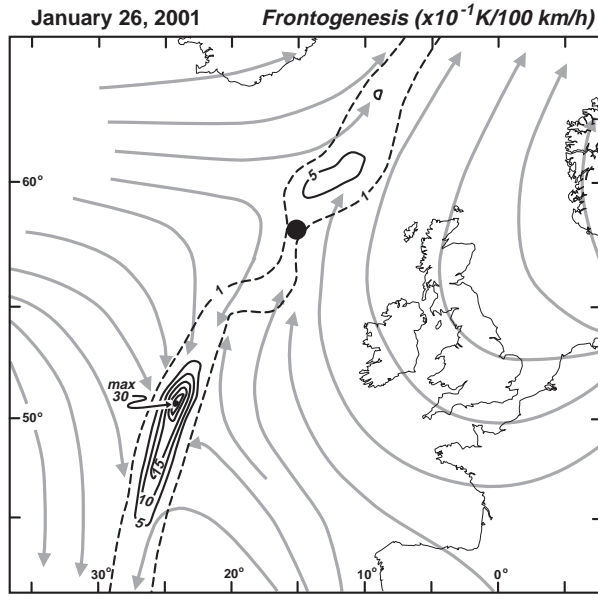


Fig. 2. Streamline analysis at 00 UTC 26 January 1997 superimposed on the frontogenesis calculations. The black dot represents the location of the front that was sampled by the Electra.

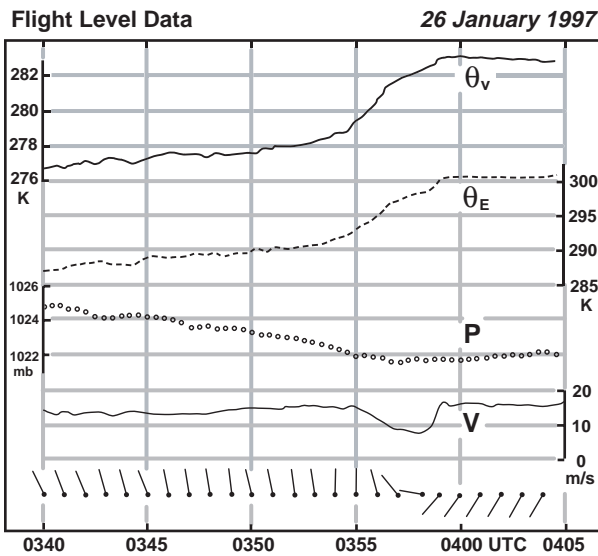


Fig. 3. Time series of in situ data from 0340 - 0405 UTC.

in Fig. 4. The shift from strong southwesterly flow in the warm sector to northerly flow in the cold sector is apparent.

3. VERTICAL CROSS SECTIONS

The vertical structure of the front is revealed in cross sections oriented perpendicular to the frontal boundary (Fig. 5). The front is rather shallow and is well-defined by the packing and sloping isentropes as well as the wind shift shown in Fig. 5a. Indeed, the cold pool is less than 2 km in depth at a distance of ~ 140 km to the west of the surface position of the front. Radar reflectivities are

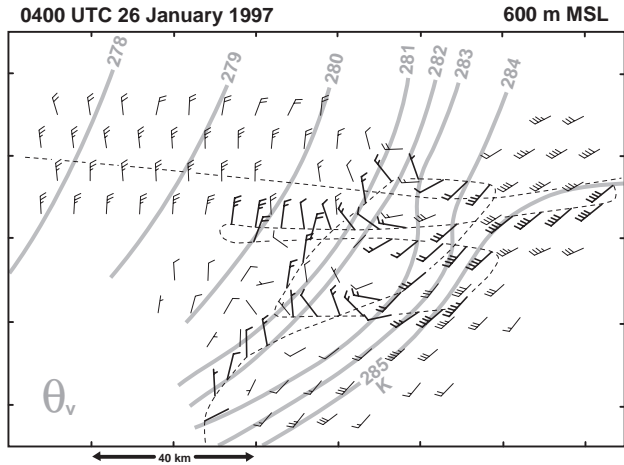


Fig. 4. Plot of virtual potential temperature at 600 m AGL combined with dual-Doppler and in situ winds at flight level. The flight track of the Electra is shown by the dashed line.

greater than 10 dBZ at the leading edge of the front (Fig. 5b) and the vertical velocities (not shown) are weak. Weak bands of echoes were resolved within the cold air with their axis aligned parallel to the orientation of the surface front. Two of these weak bands (reflectivities >5 dBZ) can be seen in Fig. 5b. The maximum vertical vorticity exceeds $1 \times 10^{-3} \text{ s}^{-1}$ but does not extend far behind the position of the surface front.

The semigeostrophic model of frontogenesis is the main theoretical framework in which frontal dynamics is described (e.g., see Hoskins 1982). The front is treated as a quasi-two-dimensional flow in which there is a close degree of geostrophic balance in the along-front direction. The degree of along-front thermal wind balance (TWI) is related to the accuracy of the semigeostrophic model. TWI does not need to be zero but it should be small and will be related to the cross-frontal ageostrophic circulation.

The analysis of TWI is shown in Fig. 5c. Negative values means that the actual wind is less than the geostrophic wind based on thermal wind balance across the front. This may indicate a region where the front is undergoing active frontogenesis or there is diabatic forcing present.

4. SUMMARY

The present case illustrates one of the rare opportunities to investigate the characteristics of a front positioned within a horizontal deformation field. The front was defined by a distinct wind shift of almost 180° and a strong temperature gradient. Vertical cross sections revealed that the cold front was well-defined but shallow. Active frontogenesis appeared to be concentrated at the surface position of the front based on TWI which was also confirmed by the synoptic scale analysis.

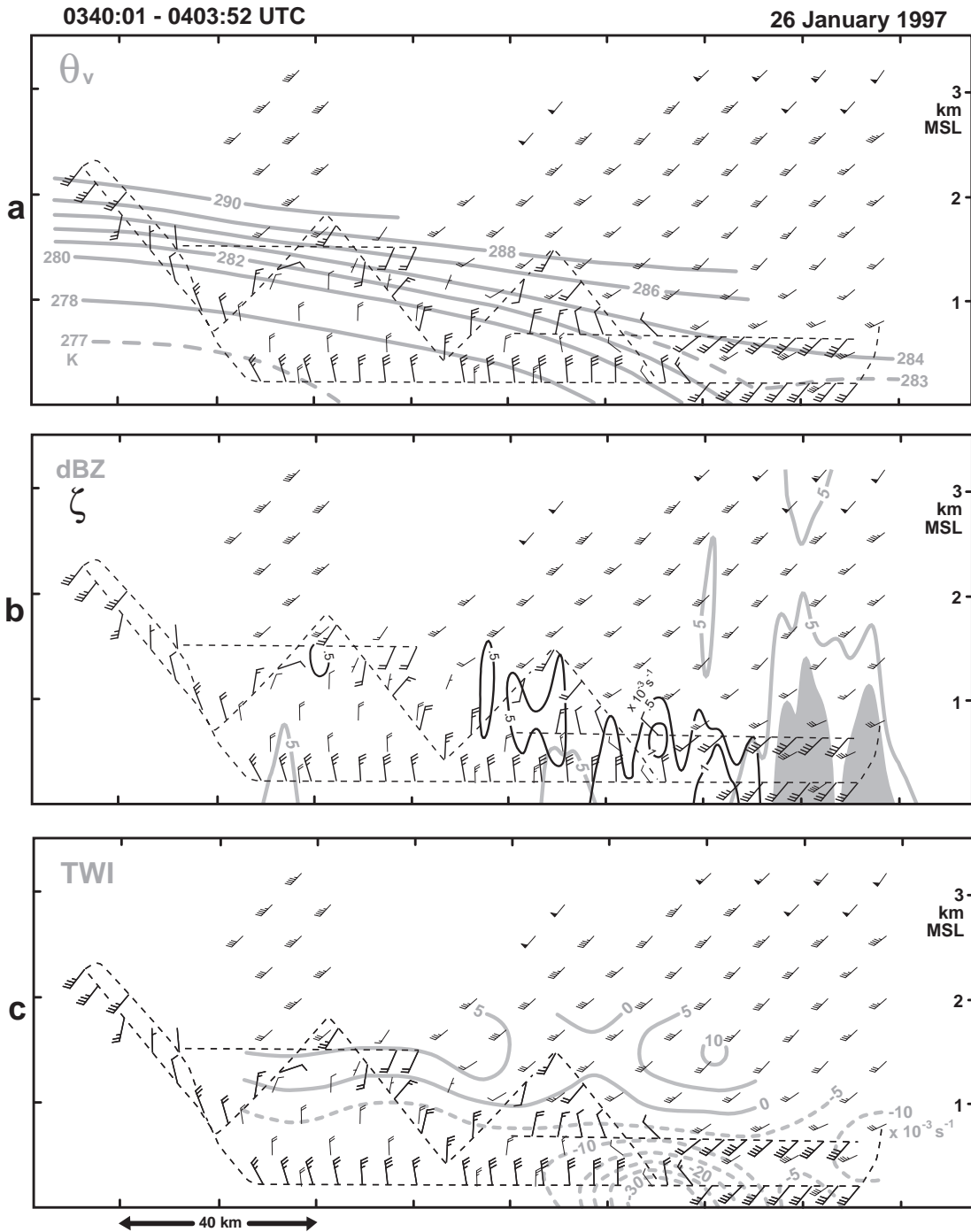


Fig. 5. Mean vertical cross sections of a) virtual potential temperature, b) vertical vorticity and radar reflectivity, and c) thermal wind imbalance. Ground-relative dual-Doppler and in situ winds are also plotted. The flight track of the Electra is shown by the dashed line.

Acknowledgments: Research results presented in this paper were supported by the National Science Foundation under Grants ATM 9801720.

References

Davies, H.C., and J.C. Müller, 1988: Detailed description of deformation-induced semigeostrophic frontogenesis. *Quart. J. Roy. Meteor. Soc.*, **114**, 1201-1219.

Holton, J.R., 1992: *An introduction to dynamic meteorology*. Academic Press, New York, 511 pp.

Hoskins, B.J., 1982: The mathematical theory of frontogenesis. *Ann. Rev. Fluid Mech.*, **14**, 131-151.

Ostdiek, V., and W. Blumen, 1995: Deformation frontogenesis: Observations and theory. *J. Atmos. Sci.*, **52**, 1487-1500.